Supporting information for

Nanometer-Scale Separation of d^{10} Zn^{2+}-Layers and Twin-Shift Competition in $Ba_8ZnNb_6O_{24}$-Based 8-Layer Hexagonal Perovskites

Fengqi Lu,[1] Xiaoming Wang,[2] Zhengwei Pan,[3] Fengjuan Pan,[3] Shiqiang Chai,[3] Chaolun Liang,[4] Quanchao Wang,[1] Jing Wang,[3] Liang Fang,[1] XiaojunKuang[1,3,*], Xiping Jing[2,*]

1. *Guangxi Ministry-Province Jointly-Constructed Cultivation Base for State Key Laboratory of Processing for Nonferrous Metal and Featured Materials, Guangxi Universities Key Laboratory of Non-ferrous Metal Oxide Electronic Functional Materials and Devices, College of Materials Science and Engineering, Guilin University of Technology, Guilin 541004 P. R. China*
2. *Beijing National Laboratory for Molecular Sciences, The State Key Laboratory of Rare Earth Materials Chemistry and Applications, College of Chemistry and Molecular Engineering, Peking University, Beijing 100871, P. R. China*
3. *MOE Key Laboratory of Bioinorganic and Synthetic Chemistry, State Key Laboratory of Optoelectronic Materials and Technologies, School of Chemistry and Chemical Engineering, Sun Yat-Sen University, Guangzhou 510275, P. R. China*
4. *Instrumental Analysis and Research Center, Sun Yat-Sen University, Guangzhou 510275, P. R. China*

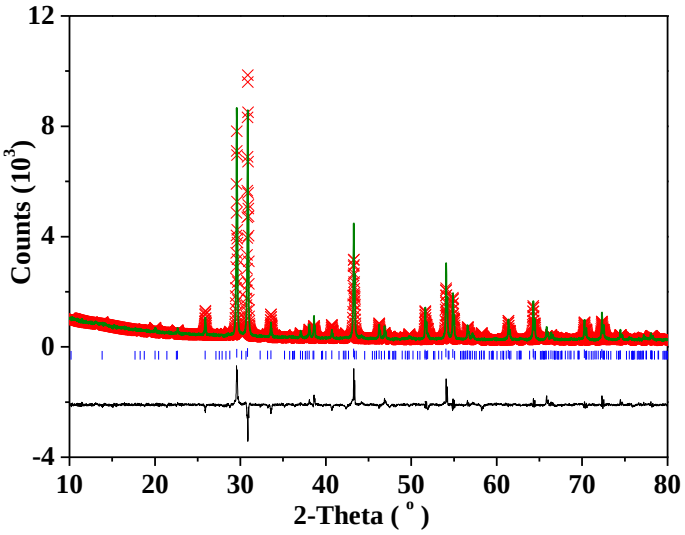

Figure S1. Rietveld refinement plot of XRD data for $Ba_8ZnNb_6O_{24}$ based on the twinned structure.

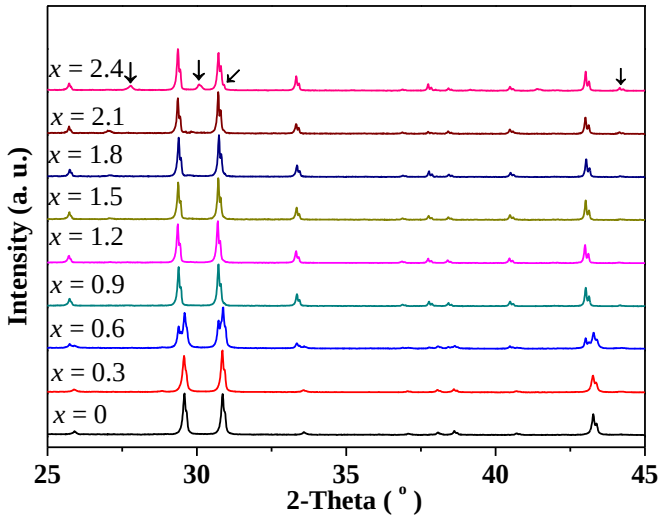

Figure S2. XRD patterns of $Ba_8ZnNb_{6-x}Sb_xO_{24}$ (x = 0, 0.3, 0.6, 0.9, 1.2, 1.5, 1.8, 2.1, 2.4). The arrows denote the reflections from the impurities.

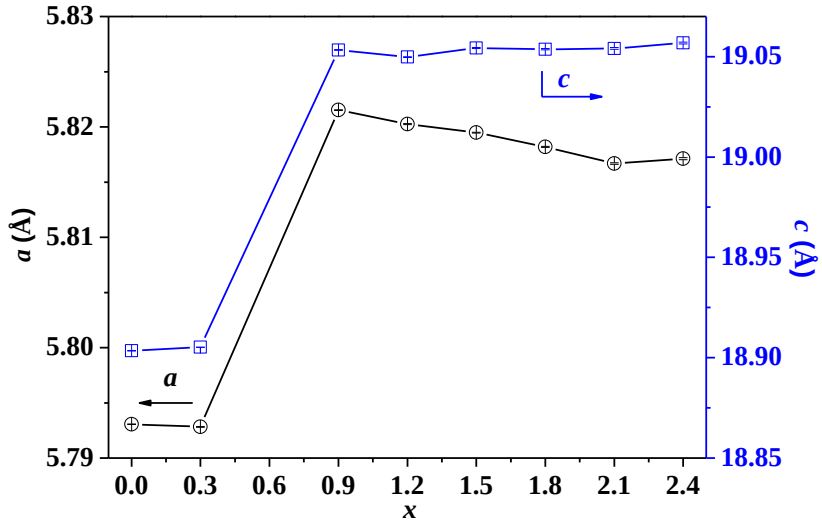

Figure S3. Refined cell parameters *a* and *c* of $Ba_8ZnNb_{6-x}Sb_xO_{24}$ (*x* = 0, 0.3, 0.9, 1.2, 1.5, 1.8, 2.1 2.4) based on the unit cell of shifted $Ba_8ZnNb_6O_{24}$ structure.

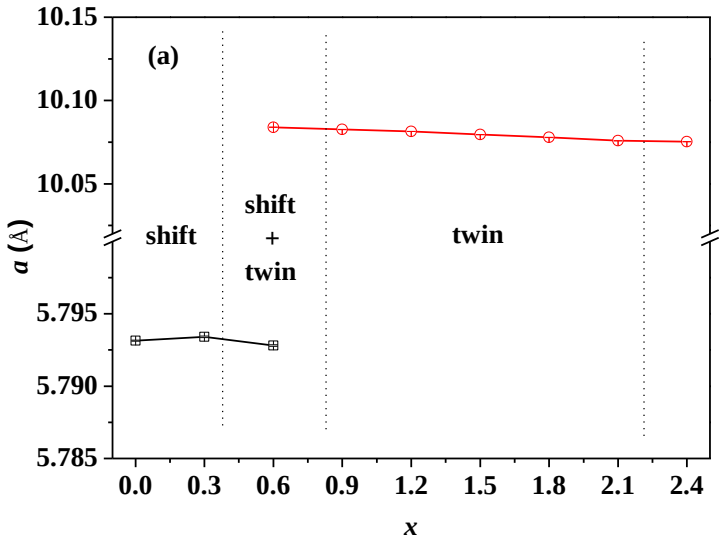

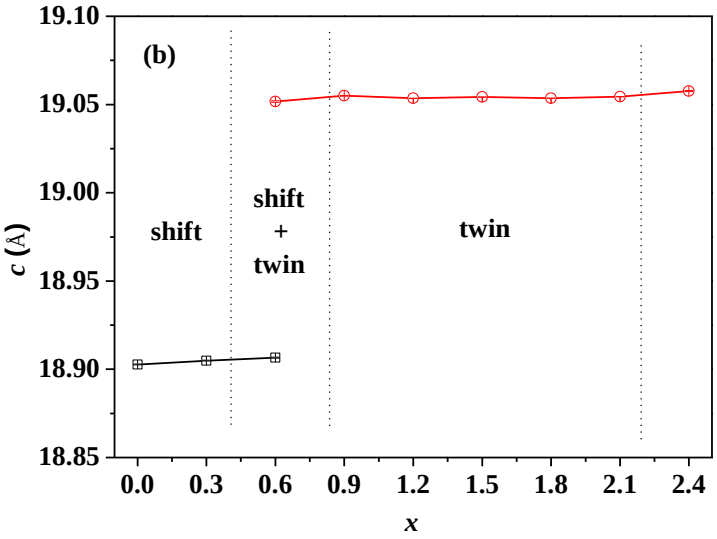

Figure S4. Refined cell parameters *a* (a) and *c* (b) of the twined and shifted phases in $Ba_8ZnNb_{6-x}Sb_xO_{24}$ (x = 0, 0.3, 0.9, 1.2, 1.5, 1.8, 2.1, 2.4).

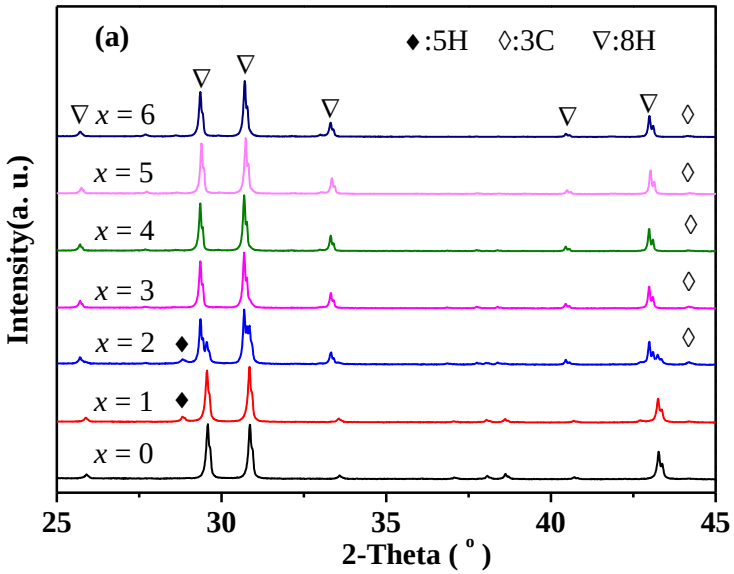

Figure S5. XRD patterns of $Ba_8ZnNb_{6-x}Ta_xO_{24}$ (x = 0, 1, 2, 3, 4, 5, 6) in 2Theta range 25-45°.

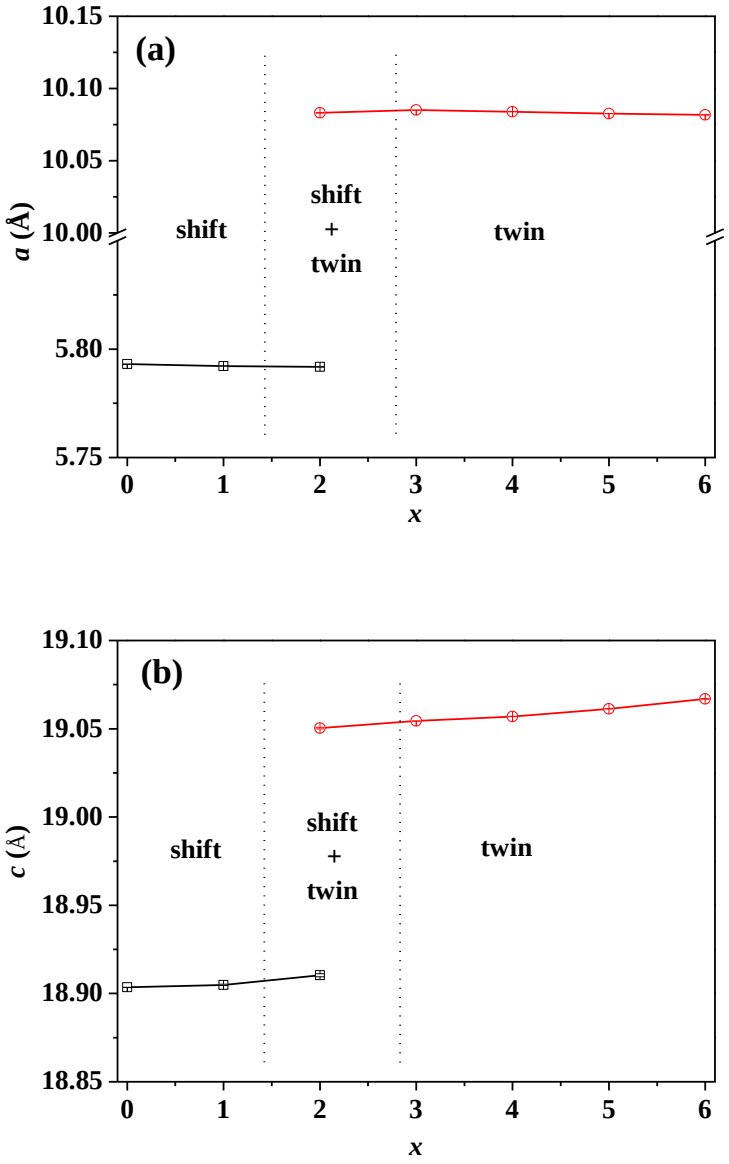

Figure S6. Refined cell parameters *a* (a) and *c* (b) of the twinned and shifted phases in $Ba_8ZnNb_{6-x}Ta_xO_{24}$ (x = 0, 1, 2, 3, 4, 5 and 6).

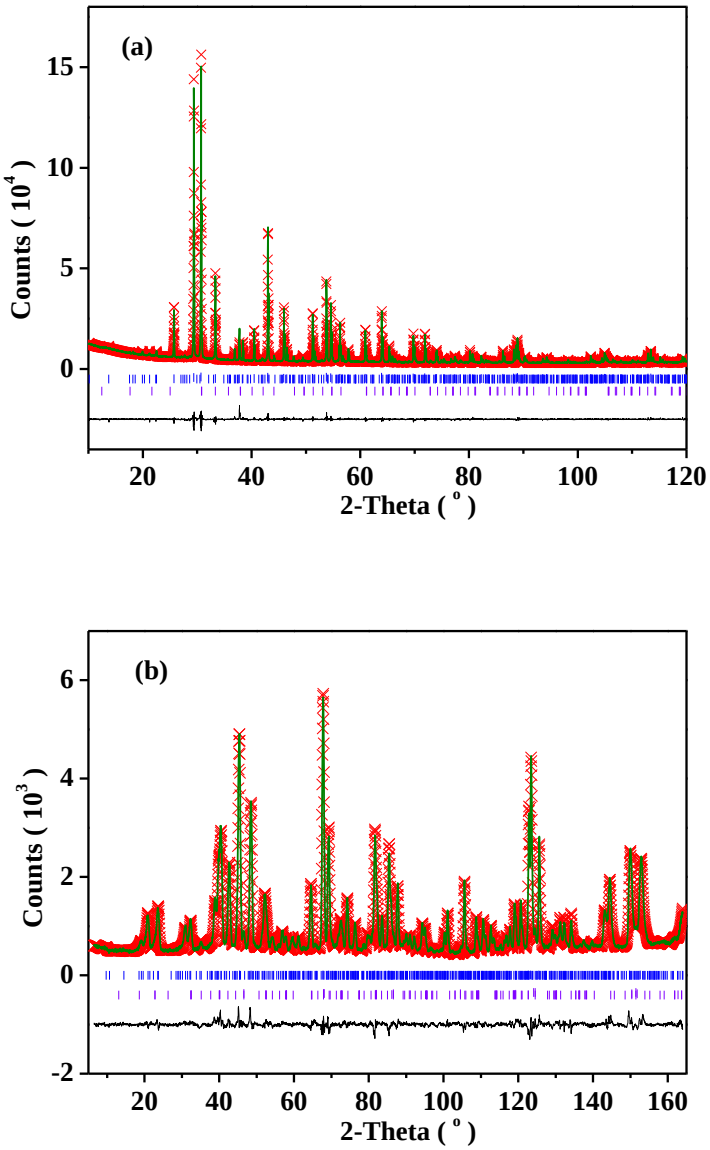

Figure S7. Rietveld plots of XRD (a) and NPD (b) data for the twinned $Ba_8ZnNb_{5.1}Sb_{0.9}O_{24}$. Vertical tick marks from top to bottom represent Bragg reflection positions of $Ba_8ZnNb_{5.1}Sb_{0.9}O_{24}$ and $Ba_3ZnNb_2O_9$, and their refined weight percentages are 97.49(7) wt% and 2.51(7) wt%, respectively.

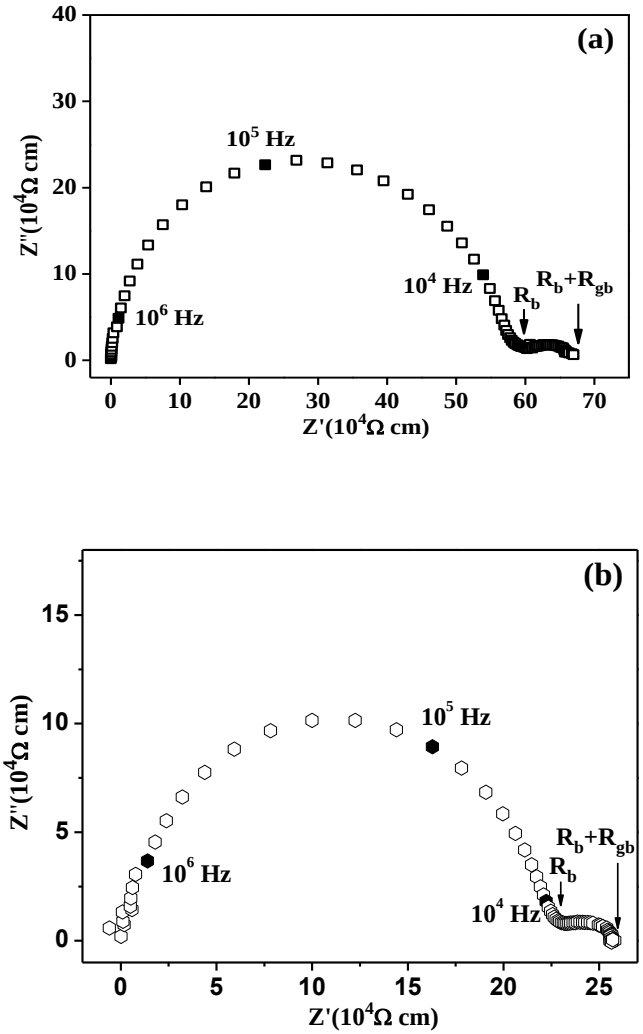

Figure S8. Complex impedance plot of $Ba_8ZnNb_6O_{24}$ (a) and $Ba_8ZnNb_{5.1}Sb_{0.9}O_{24}$ (b) pellets at 800 °C. R_b and R_{gb} denote bulk and grain boundary resistivity, respectively. The selected frequencies were marked by the filled symbols.

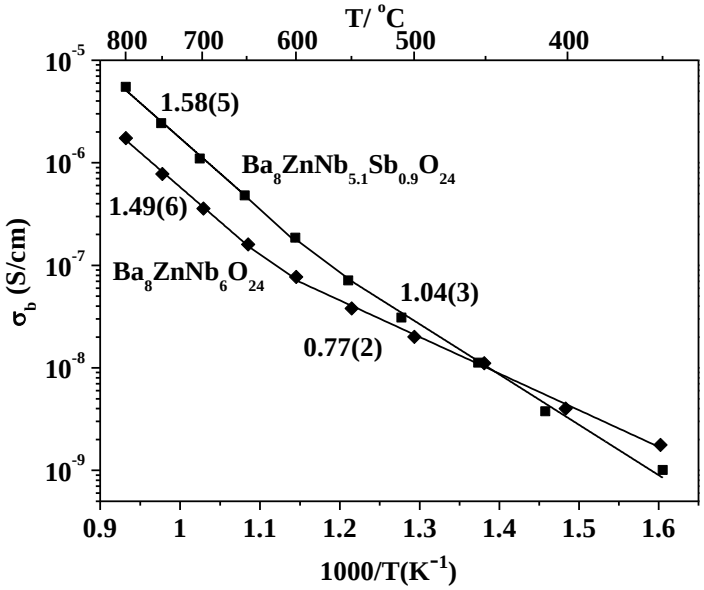

Figure S9. Arrhenius plots of bulk conductivity of the $Ba_8ZnNb_6O_{24}$ and $Ba_8ZnNb_{5.1}Sb_{0.9}O_{24}$ pellets. The activation energies (eV) are marked in the low and high temperature regions for each pellet.

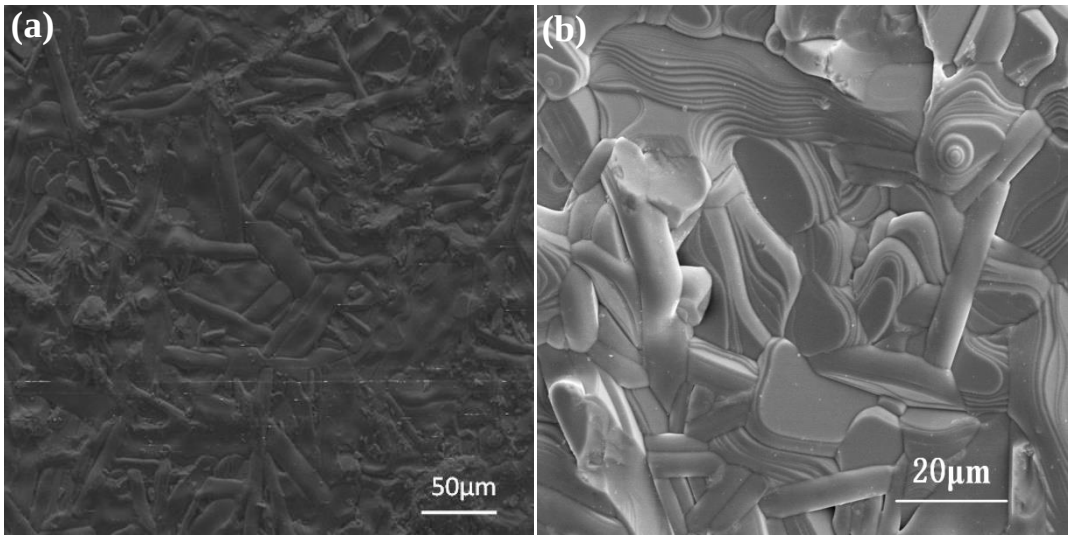

Figure S10. SEM images of the $Ba_8ZnNb_6O_{24}$ (a) and $Ba_8ZnNb_{5.1}Sb_{0.9}O_{24}$ (b) pellets.

Table S1. Interatomic distances, octahedral distortion parameters (Δd^*) and B-O-B angles for twinned $Ba_8ZnNb_{5.1}Sb_{0.9}O_{24}$.

Bond	Length(Å)	Bond	Length (Å)/Angles (°)
Ba1-O2(×3)	2.734(6)	Zn1-O4(×3)	2.157(4)
Ba1-O5(×6)	2.917(7)	Zn1-O8(×3)	2.151(2)
Ba1-O7(×3)	3.142(2)	Δd_{Zn1} (10^{-6})	1.9
Ba2-O8(×3)	2.890(1)	Nb2/Sb2-O4(×3)	1.878(4)
Ba2-O1(×3)	2.9108(4)	Nb2/Sb2-O6(×3)	2.214(3)
Ba2-O6(×3)	2.763(2)	$\Delta d_{Nb2/Sb2}$ (10^{-3})	6.7
Ba2-O5(×3)	2.907(6)	Nb3/Sb3-O3(×3)	1.955(4)
Ba3-O6(×2)	2.861(4)	Nb3/Sb3-O7(×3)	2.184(2)
Ba3-O4(×2)	2.636(1)	$\Delta d_{Nb3/Sb3}$ (10^{-3})	3.1
Ba3-O5(×2)	3.033(1)	Nb4 -O7(×1)	1.940(3)
Ba3-O7(×2)	2.952(7)	Nb4-O6(×2)	1.927(3)
Ba3-O1(×1)	3.039(4)	Nb4-O5(×2)	2.073(2)
Ba3-O6(×2)	2.972(2)	Nb4-O1(×1)	2.060(7)
Ba3-O3(×1)	2.804(3)	Δd_{Nb4} (10^{-3})	1.2
Ba4-O3(×1)	2.798(3)	Nb5-O8(×2)	1.978(1)
Ba4-O2(×2)	2.835(2)	Nb5-O1(×1)	2.015(7)
Ba4-O8(×2)	2.799(8)	Nb5-O5(×2)	2.066(1)
Ba4-O4(×2)	2.956(1)	Nb5-O2(×1)	1.966(8)
Ba4-O8(×2)	3.159(9)	Δd_{Nb5} (10^{-4})	4.2
Ba4-O5(×2)	3.111(1)	Nb6/Sb6-O2(×3)	1.884(8)
Ba4-O1(×1)	3.169(4)	Nb6/Sb6-O3(×3)	2.351(7)
Ba5-O7(×1)	2.776(3)	$\Delta d_{Nb6/Sb6}$ (10^{-2})	1.2
Ba5-O4(×2)	2.893(5)	Zn1-O4-Nb2/Sb2	70.29(6)
Ba5-O6(×2)	3.073(1)	Zn1-O8-Nb5/Sb5	172.57(5)
Ba5-O3(×2)	2.920(8)	Nb3-O3-Nb6/Sb6	85.10(6)
Ba5-O2(×1)	3.024(6)	Nb2/Sb2-O6-Nb4	170.47(6)
Ba5-O8(×2)	2.943(1)	Nb3-O7-Nb4	171.03(7)
Ba5-O4(×2)	2.940(3)	Nb4-O1-Nb5	178.48(8)
		Nb4-O5-Nb5/Sb5	178.23(5)
		Nb5/Sb5-O2-Nb6/Sb6	174.53(9)

Table S2. Twin-shift option, average B-cationic sizes (<R_B>), and the tolerance factors (*t*) of the B-site deficient 8-layer hexagonal perovskites $Ba_8B_7O_{24}$.

Composition	<R_B> / Å	*t*	Structure type	Ref.
$Ba_8ZnNb_6O_{24}$	0.654	1.0362	Shifted	This work
$Ba_8ZnNb_{5.7}Sb_{0.3}O_{24}$	0.653	1.0371	Shifted	This work
$Ba_8ZnNb_{5.4}Sb_{0.6}O_{24}$	0.651	1.0380	Mixed	This work
$Ba_8ZnNb_{5.1}Sb_{0.9}O_{24}$	0.649	1.0388	Twinned	This work
$Ba_8ZnNb_5TaO_{24}$	0.654	1.0362	Shifted	This work
$Ba_8ZnNb_4Ta_2O_{24}$	0.654	1.0362	Mixed	This work
$Ba_8ZnNb_3Ta_3O_{24}$	0.654	1.0362	Twinned	This work
$Ba_8ZnTa_6O_{24}$	0.654	1.0362	Twinned	1, 2
$Ba_8Ti_3Nb_4O_{24}$	0.625	1.0511	Twinned	3
$Ba_8Ti_{2.75}Nb_{4.125}Lu_{0.125}O_{24}$	0.630	1.0484	Twinned	4
$Ba_8Ti_{2.5}Nb_{4.25}Lu_{0.25}O_{24}$	0.635	1.0457	Mixed	4
$Ba_8Ti_2Nb_{4.5}Lu_{0.5}O_{24}$	0.646	1.0404	Shifted	4
$Ba_8Ti_2Nb_{4.5}Yb_{0.5}O_{24}$	0.646	1.0403	shifted	5
$Ba_8Ti_3Ta_4O_{24}$	0.625	1.0511	twinned	6
$Ba_8CoTa_6O_{24}$	0.641	1.0427	Twinned	7
$Ba_8CoNb_6O_{24}$	0.641	1.0427	Shifted	8
$Ba_8NiTa_6O_{24}$	0.647	1.0398	Twinned	9

References:

1. Moussa, S. M.; Claridge, J. B.; Rosseinsky, M. J.; Clarke, S.; Ibberson, R. M.; Price, T.; Iddles, D. M.; Sinclair, D. C., *Appl. Phys. Lett.* **2003,** 82, 4537-4539.

2. Thirumal, M.; Davies, P. K., *J. Am. Ceram. Soc.* **2005,** 88, 2126-2128.

3. Teneze, N.; Boullay, P.; Petricek, V.; Trolliard, G.; Mercurio, D., *Solid State Sci.* **2002,** 4, 1129-1136.

4. Trolliard, G.; Teneze, N.; Boullay, P.; Mercurio, D., *J. Solid State Chem.* **2004,** 177, 1188-1196.

5. B. Mössner; Kemmler-Sack, S., *J. Less-Common Met.* **1986,** 120, 203-211.

6. Shpanchenko, R. V.; Nistor, L.; Vantendeloo, G.; Vanlanduyt, J.; Amelinckx, S.; Abakumov, A. M.; Antipov, E. V.; Kovba, L. M., *J. Solid State Chem.* **1995,** 114, 560-574.

7. Kan, A.; Ogawa, H.; Yokoi, A.; Ohsato, H., *Jpn. J. Appl. Phys.* **2006,** 45, 7494-7498.

8. Mallinson, P. M.; Allix, M. M. B.; Claridge, J. B.; Ibberson, R. M.; Iddles, D. M.; Price, T.; Rosseinsky, M. J., *Angew. Chem. Int. Ed.* **2005,** 44, 7733-7736.

9. Abakumov, A. M.; Tendeloo, G. V.; Scheglov, A. A.; Shpanchenko, R. V.; Antipov, E. V., *J. Solid State Chem.* **1996,** 125, 102-107.